Time-slice velocity-map ion imaging studies of the photodissociation of NO in the vacuum ultraviolet region

Hong Gao, Yang Pan, Lei Yang, Jingang Zhou, C. Y. Ng, and William M. Jackson

Citation: The Journal of Chemical Physics **136**, 134302 (2012); doi: 10.1063/1.3696897
View online: http://dx.doi.org/10.1063/1.3696897
View Table of Contents: http://scitation.aip.org/content/aip/journal/jcp/136/13?ver=pdfcov
Published by the AIP Publishing

Time-slice velocity-map ion imaging studies of the photodissociation of NO in the vacuum ultraviolet region

Hong Gao,[1] Yang Pan,[1,2] Lei Yang,[1] Jingang Zhou,[1] C. Y. Ng,[1] and William M. Jackson[1,a)]
[1]*Department of Chemistry, University of California, Davis, California 95616, USA*
[2]*National Synchrotron Radiation Laboratory, University of Science and Technology of China, Hefei, Anhui 230029, People's Republic of China*

(Received 2 November 2011; accepted 2 March 2012; published online 2 April 2012)

The time-slice velocity-map ion imaging and the resonant four-wave mixing techniques are combined to study the photodissociation of NO in the vacuum ultraviolet (VUV) region around 13.5 eV above the ionization potential. The neutral atoms, i.e., $N(^2D^o)$, $O(^3P_2)$, $O(^3P_1)$, $O(^3P_0)$, and $O(^1D_2)$, are probed by exciting an autoionization line of $O(^1D_2)$ or $N(^2D^o)$, or an intermediate Rydberg state of $O(^3P_{0,1,2})$. Old and new autoionization lines of $O(^1D_2)$ and $N(^2D^o)$ in this region have been measured and newer frequencies are given for them. The photodissociation channels producing $N(^2D^o) + O(^3P)$, $N(^2D^o) + O(^1D_2)$, $N(^2D^o) + O(^1S_0)$, and $N(^2P^o) + O(^3P)$ have all been identified. This is the first time that a single VUV photon has been used to study the photodissociation of NO in this energy region. Our measurements of the angular distributions show that the recoil anisotropy parameters (β) for all the dissociation channels except for the $N(^2D^o) + O(^1S_0)$ channel are minus at each of the wavelengths used in the present study. Thus direct excitation of NO by a single VUV photon in this energy region leads to excitation of states with Σ or Δ symmetry ($\Delta\Omega = \pm 1$), explaining the observed perpendicular transition. © *2012 American Institute of Physics*. [http://dx.doi.org/10.1063/1.3696897]

I. INTRODUCTION

Nitric oxide has been one of the most extensively studied diatomic molecules during the past 70 years. The unpaired electron in the ground electronic state makes it interesting to study because its electronic structure makes it a prototype for other open shell molecules. From the practical point of view, nitric oxide is an important molecule in the upper atmosphere where it contributes to the destruction of the ozone layer,[1,2] and it is an important pollution gas in the thermosphere.[3] Nitric oxide has also been found in the interstellar medium,[4] where it can react with $N(^4S)$ at low temperatures to produce $N_2(^1\Sigma_g^+)$.[5] There is one unpaired electron in the highest occupied molecular orbital (HOMO) anti-bonding π^* orbital that makes it difficult to study theoretically. Miescher and Dressler measured the high-resolution absorption spectra of NO in the region above and below the first ionization threshold in an effort to obtain a clearer picture of the adiabatic and diabatic potential energy curves of NO.[6–8] They identified several electronic valence and low-lying Rydberg states as well as their mutual interactions. The complicated potential curves of NO in this region and their mutual interactions did not become clearer or more quantitative without several additional theoretical studies. Gallusser and Dressler made great theoretical progress by identifying the homogeneous Π-Π interactions in this region.[9] Vivie and Peyerimhoff employed the multi-reference configurations interaction (MRCI) method and studied all the valence states and some of the low-lying Rydberg states. They obtained quantitative results for both the adiabatic and diabatic potential energy curves of NO in this region.[10] Polak and Fiser[11] and Shi and East[12] recently improved upon these results. Thanks to these experimental and theoretical efforts, the potential energy curves of NO below the first ionization threshold are well understood.

In the energy region above the first ionization threshold, the potential energy curves are still not well known. Only a few theoretical calculations have been done in this region even though there have been many experimental investigations. The first study of the absorption coefficients of nitric oxide in the vacuum ultraviolet (VUV) region was reported in 1955 by Sun and Weissler[13] and later by Metzger *et al.*[14] and Watanabe *et al.*[15] with higher energy resolution. In the vacuum ultraviolet (VUV) region above the IE of nitric oxide, there are many Rydberg series, which converge to excited states of NO^+.[16] More recent high resolution photoabsorption, photoionization, and electron energy-loss studies from its ionization threshold to about 30 eV have been done and several Rydberg series were identified.[17–21] Jarvis *et al.* have reported on the rotational resolved PFI-PE spectra for NO^+ ($X^1\Sigma^+$, $v^+ = 0$–32) and NO^+ ($a^3\Sigma^+$, $v^+ = 0$–16).[22,23] A recent review of the photoabsorption and photoionization of NO over a very large energy range was included in the book of Berkowitz.[24]

Photodissociation of nitric oxide has been the topic for several studies. Direct detection of $N(^2D^o)$ using REMPI to study the two-photon NO photodissociation was first reported from the dissociation threshold to its ionization limit[25] and then above the ionization limit[26] by Gadd *et al.*, and later on by Fujii and Morita.[27–29] In the latter studies both the $N(^2D^o)$ and $N(^4S^o)$ fragments were probed. They investigated

a)Author to whom correspondence should be addressed. Electronic mail: wmjackson@ucdavis.edu.

the competition between photoionization and photodissociation for the super-excited Rydberg states. The newly developed velocity-map ion imaging technique has been applied to the photodissociation study of NO by Bakker *et al.*[30,31] and Cosofret *et al.*[32] Here again a two-photon excitation scheme was used for their investigations. The dissociation channels producing $N(^4S^o) + O(^3P)$ and $N(^2D^o) + O(^3P)$ were identified from the translational energy release spectra, their angular distributions and branching ratios were measured at the same time. Besides these two-photon excitation studies of the laser photodissociation of NO in the vicinity of its first ionization threshold, several other studies[19,33–36] have focused on the photoionization and predissociation of NO in the vacuum ultraviolet region above 16 eV using the synchrotron radiation. In this high energy region, highly excited electronic photofragments can be formed from the predissociation process and the fluorescence from these fragments was measured as a function of the excitation energy. When even higher excitation energies are used, ion pairs can be formed[19,37] and the dissociative ionization[19,36,38] process can be studied.

Compared with the studies described above, there have been very few direct photodissociation studies in the energy region between them, i.e., around 13.5 eV. In fact, this is the region with the strongest absorption in the NO absorption spectrum,[13,14,18] a strong broadened dissociation band centered at about 13.5 eV has been predicted by Metzger *et al.*[14] There are two reasons why there are very few photodissociation studies in this energy region. First, it is not easy to generate radiation in this region with narrow enough bandwidth and high enough intensity. Second, probing the photofragment is not trivial because fragment fluorescence is weak since the excited fragments in this energy region are metastable with long fluorescence lifetimes. Yet it is important to understand the details of the photodissociation dynamics of NO in this energy region, i.e., the electronic states, kinetic energy, and angular distributions of the atomic fragments. This energy region is right below the IE of the hydrogen atom, which is about 13.6 eV. Interstellar radiation below this energy can penetrate dense interstellar clouds and protoplanetary nebula. Photodissociation studies of NO in this region are important for understanding the properties of the planetary atmospheres and the interstellar medium because of the relative large absorption and photodissociation cross sections of NO in this region.[14] At the same time, direct photodissociation measurements of NO in this region, i.e., the product channels and their angular distributions, can provide useful information for comparison with theoretical calculations. We have recently combined the time-slice velocity-map ion imaging technique with resonant sum or difference four-wave mixing technique in rare gases to study the photodissociation dynamics of small molecules in the vacuum ultraviolet (VUV) region.[39,40] The translational energy and angular distributions of the fragments were determined from the ion images. That work showed that many product channels that are forbidden by the Wigner-Witmer selection rules[41] can be formed in the vacuum ultraviolet (VUV) region. In this paper, we describe time-slice velocity-map ion images of the photofragments produced from the photodissociation of NO at several of the autoionization lines or Rydberg states of nitrogen and oxygen atoms near 13.5 eV using only one windowless VUV generation system. To the best of our knowledge, this is the first direct one-photon photodissociation study of NO in this energy region.

II. EXPERIMENT

A detailed description of the laser photodissociation time-slice velocity-map ion-imaging apparatus has been previously reported[42,43] and will only be briefly summarized here. A pulsed molecular beam of less than 5% NO seeded in He is produced by supersonic expansion through an Even-Lavie pulsed valve (EL-5-2004). The nozzle diameter of the valve is 0.2 mm and it is operated at 30 Hz with a stagnation pressure of 50 psi. The pulsed beam is skimmed by two conical skimmers prior to entering the photodissociation/photoionization (PD/PI) region where it is intersected by the VUV photodissociation and photoionization laser at 90°. The distance between the nozzle and the interaction region is ~15 cm. The ions produced by VUV laser photoionization of the nascent photofragments and the parent molecules are extracted and focused by the velocity-map ion optics onto a 7.5 cm micro-channel plate (MCP) detector. The electrons from this detector are accelerated to a phosphor screen where the image is recorded by a CCD camera.

The tunable VUV laser radiation generation system has also been previously described.[44] In this study, the tunable VUV laser radiation was generated by resonant nonlinear four-wave sum-frequency ($2\omega_1 + \omega_2$) mixing using Kr gas as the nonlinear medium, where ω_1 and ω_2 are the UV and visible laser frequencies, respectively. The ω_1 and ω_2 radiations are generated by two dye lasers (Lambda Physik, FL3002) that are pumped by the second harmonic output of the same Nd:YAG laser (Spectra Physics PRO-290) operated at 30 Hz. The ω_1 fundamental wavelength was fixed at 212.556 nm to coincide with the two-photon transition process $4s^24p^5(^2P_{3/2})5p'[1/2](J = 0) \leftarrow 4s^24p^6(^1S_0)$ of Kr at 94 092.86 cm^{-1}. The ω_1 frequency is generated by doubling the fundamental output of the dye laser at 637.668 nm with a BBO crystal cut at an angle of 37.4° and then summing the second harmonic output from the first BBO crystal with the fundamental output of the dye laser using a second BBO crystal cut at an angle of 69°. A dichroic mirror merges the ω_1 and ω_2 beams before entering the nonlinear mixing chamber through a fused silica window. The Kr gas was expanded into a T-shaped channel by a pulsed valve (General Valve) operated at 30 Hz. The four-wave mixing process generates three VUV beams at $2\omega_1 + \omega_2$, $2\omega_1 - \omega_2$, and $3\omega_1$ when the ω_1 and ω_2 beams are focused into a spot of the T-shaped channel that is 27.3 cm away from the interaction region. There is no separation lens between this T-shaped channel and the PD/PI region so that the VUV, UV, and visible laser beams all enter the interaction region after passing through a 2 mm aperture. All of the images in the present study were obtained by using the autoionization lines of the $N(^2D)$, $O(^1D)$, and the intermediate Rydberg states of the $O(^3P_{0,1,2})$ atoms. As a result, the photodissociation wavelengths are limited to the wavelengths associated with these lines. The VUV light is scanned back and forth over the Doppler profile of the atomic line of the

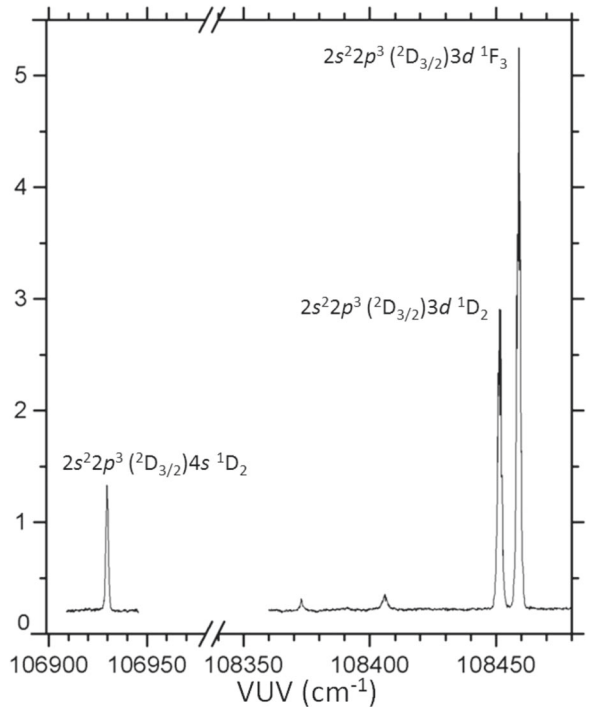

FIG. 1. The VUV spectrum of O^+ produced by exciting the autoionization lines of $O(^1D)$ produced from the photodissociation of NO. The VUV wavelength was scanned from 106 900 cm^{-1} to 108 480 cm^{-1}. The relative intensity is not normalized to the VUV intensity and the two parts of the spectrum were scanned separately (this range cannot be covered with only one visible laser dye). The VUV photon energy is calculated by $2\omega_1 + \omega_2$. The assignments for each of the three strong peaks are showed in the figure.

product atom by tuning the visible dye laser ω_2 while accumulating the images.

III. EXPERIMENTAL RESULTS

A. Detection of the $O(^1D_2)$ fragment

A single-photon ionization study of atomic oxygen $O(^1D_2)$ between 12 and 18 eV has been previously reported by Flesch *et al.*[45] In that study, two autoionization peaks of $O(^1D_2)$ were observed at 13.26 and 13.45 eV. In the present study NO is used as the precursor to produce $O(^1D_2)$ and by scanning the VUV radiation from 106 900 cm^{-1} to 108 480 cm^{-1}, the autoionization spectrum of $O(^1D_2)$ is reproduced in Fig. 1. From the spectrum, we can see that the strong peak assigned to the n*d* series converging to $O^+(^2D^o)$ seen at 13.45 eV in Ref. 45 turns out to be two strong peaks that are very close to each other. Their wavelengths occur at 108 451.5 cm^{-1} (13.4463 eV) and 108 459.0 cm^{-1} (13.4472 eV) and they have been assigned to the $2s^22p^3\ (^2D_{3/2})3d\ ^1D_2 \leftarrow O(^1D_2{}^o)$ and $2s^22p^3\ (^2D_{3/2})3d\ ^1F_3 \leftarrow O(^1D_2{}^o)$ transitions, respectively. The weaker peak at 13.26 eV that is assigned to the n*s* series converging to $O^+(^2D^o)$ in Ref. 45 is observed at 106 929.8 cm^{-1} (13.2576 eV) and assigned as the $2s^22p^3\ (^2D_{3/2})4s\ ^1D_2{}^o \leftarrow O(^1D_2{}^o)$ transition. Besides the three strong autoionization peaks, two weak extra peaks are observed at 108 373.0 cm^{-1} (13.4365 eV) and 108 406.0 cm^{-1} (13.4406 eV). Using the NIST table,[46] these two peaks are assigned to the $2s^22p^3\ (^2D^o)3d\ ^3G_5{}^o \leftarrow O(^1D_2{}^o)$ and $2s^22p^3\ (^2D_{5/2}{}^o)3d\ ^1P_1{}^o \leftarrow O(^1D_2{}^o)$ transitions, respectively.

We studied the photodissociation of NO in the VUV region by tuning the sum-frequency VUV laser to one of the three strongest autoionization lines of $O(^1D_2{}^o)$ shown in Fig. 1. The time-slice velocity-map ion images of the $O(^1D_2{}^o)$ produced from the photodissociation of NO at these photon energies are then collected while scanning the laser back and forth through the Doppler profile of each of the lines. The same sum-frequency VUV beam is used to both photodissociate the NO and to photoionize the $O(^1D_2{}^o)$ fragments via an autoionization process. The images at the three wavelengths are very similar but only the one formed at the VUV energy of 108 459.0 cm^{-1} (13.4472 eV) is showed in Fig. 2(a) along with the corresponding $P(E_{TKER})$, i.e., total kinetic energy release (TKER), spectrum in Fig. 2(b) (solid curve). The $P(E_{TKER})$ spectrum at the VUV energy of 106 929.8 cm^{-1} (13.2576 eV) is given in Fig. 2(b) (dotted curve) to compare with the one measured at 108 459.0 cm^{-1} (13.4472 eV). In the $P(E_{TKER})$ spectrum at the VUV energy of 108 459.0 cm^{-1} (13.4472 eV), there is a strong peak at 2.62 eV. This corresponds to the photodissociation of NO into $N(^2D^o) + O(^1D_2{}^o)$ channel after the absorption of a

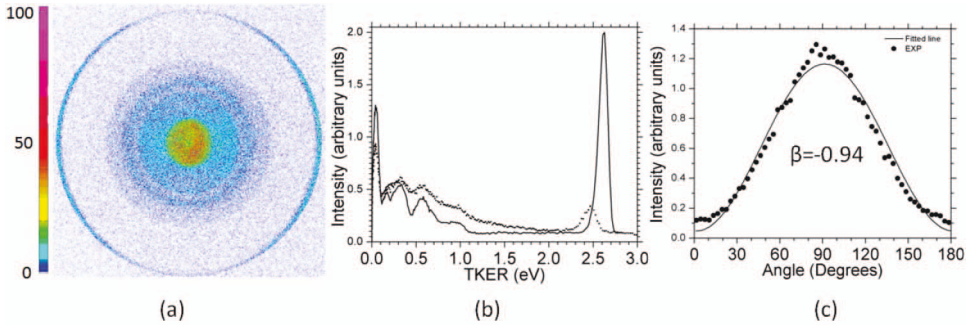

FIG. 2. Time-slice image, total kinetic energy release spectrum, and the angular distribution for photodissociation channel $N(^2D^o) + O(^1D^o)$ produced after single VUV photon excitation of NO and detection of the $O(^1D^o)$ atom at the same wavelength through an autoionization line. (a) Time-slice image at VUV photon energy of 108 459.0 cm^{-1} (13.4472 eV), (b) $P(E_{TKER})$ spectra at VUV photon energies of 108 459.0 cm^{-1} (13.4472 eV) (solid curve) and 106 929.8 cm^{-1} (13.2576 eV) (dotted curve), and (c) angular distribution of the channel $N(^2D^o) + O(^1D^o)$ produced after VUV photon excitation at 108 459.0 cm^{-1} (13.4472 eV), a recoil anisotropy parameter of −0.94 gave the best fit (solid line) to the experimental measurement (solid dots) of the angular distribution of the peak corresponding to the channel $N(^2D^o) + O(^1D^o)$.

TABLE I. Recoil anisotropy parameters for the dissociation channel $N(^2D^o) + O(^1D^o)$.

VUV photon energy (eV)	Anisotropic parameter: β[a]
13.4472	-0.8 ± 0.2[b]
13.4463	-0.8 ± 0.1
13.2576	-0.5 ± 0.3

[a]The equation $I(\theta) = (\sigma/4\pi)[1 + \beta P_2(\cos\theta)]$ was used to fit the experimental data to determine the β values.
[b]The standard deviations were generated from three independent measurements.

single VUV photon of 108 459.0 cm^{-1} (13.4472 eV). The corresponding peak is shifted to about 2.45 eV in the $P(E_{TKER})$ spectrum (dotted curve) at the VUV energy of 106 929.8 cm^{-1} (13.2576 eV). This confirms that this peak is produced by the photodissociation of NO into the channel $N(^2D^o) + O(^1D_2{}^o)$ after the absorption of a single sum-frequency VUV photon. The other energetic available dissociation channels produce $N(^4S^o) + O(^1D_2{}^o)$ and $N(^2P^o) + O(^1D_2{}^o)$ and they should have peaks in the $P(E_{TKER})$ spectrum at 4.98 eV and 1.40 eV, respectively. No peaks at these energy positions indicate that these two dissociation channels are not produced in significant amounts at 108 459.0 cm^{-1} (13.4472 eV) and at 106 929.8 cm^{-1} (13.2576 eV) by single photon absorption. The experimental angular distribution for the channel $N(^2D^o) + O(^1D_2{}^o)$ at photon energy of 108 459.0 cm^{-1} (13.4472 eV) is shown by solid dots in Fig. 2(c), and the fitted result is shown by solid line. A recoil anisotropy parameter of -0.94 was obtained from the fitting process for this single measurement which is in the error bar showed in Table I.

The low energy region of the $P(E_{TKER})$ spectra in Fig. 2(b) does not fit with any product that could come from the photodissociation of an isolated NO molecule because the energies do not correspond to any possible N atom product that can be produced any of the laser frequencies present in the interaction region. There is no way for the recoiling $O(^1D_2{}^o)$ atom to lose any translational energy in the molecular beam, therefore these atoms must be produced from the photodissociation of a NO dimer or a larger cluster containing NO. This is supported by the following experimental observation. When the percentage of NO was increased in a seeded beam with He as the carrier gas, the low energy part increased relative to the monomer peak in the $P(E_{TKER})$ spectra. This cannot happen if the low energy part is also due to the photodissociation of the monomers. In fact the low energy part cannot be well resolved unless a percentage of less than 5% was used in the molecular beam. Even though a cooler molecular beam will prefer the formation of the dimer, the dilution effect may dominate here when the percentage of NO is less than 5%. The photodissociation of NO dimer has been studied by Reisler and her co-workers[47] and more recently by Gesner *et al.*[48] at longer wavelengths and thus lower energies. According to their studies, the NO dimer can dissociate into two neutral NO fragments in either the ground or electronic excited state. It can also undergo dissociative ionization to produce one neutral NO fragment and one ionic NO fragment. One possible explanation for the low energy region of the $P(E_{TKER})$ spectra is that photodissociation of the NO dimer results in the production of $N_2O + O(^1D_2{}^o)$. To our knowledge, the dissociation of the NO dimer to these products or $NO_2 + N$ channel has never been reported. In our TOF spectrum, we see masses due to fragments of N_2O^+ and $NO_2{}^+$. This suggests the existence of two new channels, which produce $N_2O + O$ and $NO_2 + N$. Additional work is needed to understand the details of the dissociation of the NO dimer.

The recoil anisotropy parameters are measured for the $N(^2D^o) + O(^1D_2{}^o)$ dissociation channel at the three VUV wavelengths and they are listed in Table I. The standard deviations are generated from three independent measurements of these parameters. Because the signal is much weaker at the VUV photon energy of 106 929.8 cm^{-1} (13.2576 eV) for the $N(^2D^o) + O(^1D_2{}^o)$ dissociation channel, the corresponding standard deviation is larger compared with the other two. The recoil anisotropy parameter is close to -1 and nearly the same within experimental error for all the three wavelengths. This indicates that the transitions producing these channels are almost perpendicular.

B. Detection of the $N(^2D^o)$ fragment

It is not a trivial job to probe the excited states of nitrogen atoms. A REMPI probing scheme for $N(^2D^o)$ was developed by Jusinski *et al.*,[25] but to date a single photon ionization study of $N(^2D^o)$ has not been reported. Several theoretical calculations[49,50] and various experimental methods[51–53] have been done to study the autoionization of $N(^2D^o)$ and several Rydberg series that converge to the excited states of the N^+ have been identified. Due to the relative low energy resolution of these studies, the accurate peak positions and their assignments are still questionable. Previously it was showed that N_2 can produce $N(^2D^o)$ following the absorption of a single VUV laser photon for photolysis and another photon at the same wavelength for ionizing the fragment for detection.[40] One obtains the spectrum in Fig. 3 by monitoring the N^+ signal in the TOF spectrum and scanning the sum-frequency VUV light when a molecular beam of NO seeded in He was used. The peak at 110 290.8 cm^{-1} (13.6743 eV) in the spectrum is also

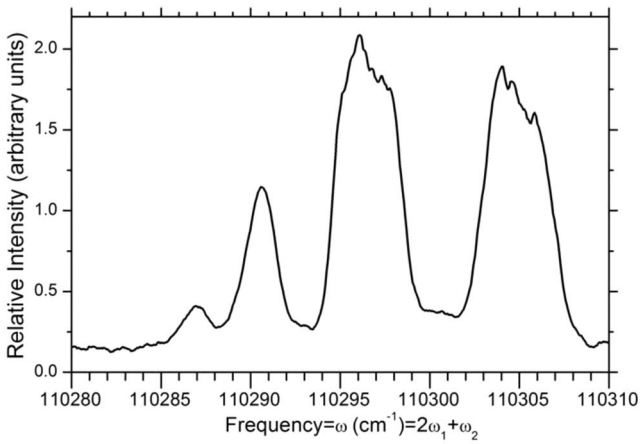

FIG. 3. VUV photoionization spectra of N atom produced from VUV photodissociation of NO from 110 280 cm^{-1} to 110 310 cm^{-1}. The relative intensity is not normalized. The peak at 110 290.8 cm^{-1} (13.6743 eV) is caused by the strong resonant line of Kr: $4s^24p^5(^2P^\circ_{3/2})8d\,^2[^1/_2]_1 \leftarrow {}^1S_0$. The Kr gas leaked into the interaction region from the VUV four-wave mixing chamber.

TABLE II. Autoionization lines of $N(^2D^o)$.

Peak position (cm^{-1})	Energy level (eV)	n^* ($^1D^e$)[b]	Possible assignment[c]
110286.7	16.0575	5.98050	$6d\ ^2D^e$, $6d\ ^2F^e$, $7s\ ^2D^e$
110296.5	16.0586	5.99007	$6d\ ^2D^e$, $6d\ ^2F^e$, $7s\ ^2D^e$
110305.0	16.0596	5.99836	$6d\ ^2D^e$, $6d\ ^2F^e$, $7s\ ^2D^e$

[a]Energy levels measured from the ground state of the nitrogen atom.
[b]Effective quantum number calculated by Rydberg formula: $E_n = IE\text{-}R/n^{*2}$.
[c]The possible assignment is made according to Refs. 49 and 52. Each of these lines can be assigned to any one of the possible Rydberg transition given in the table. A more extensive spectrum covering a larger range of wavelengths is needed to provide a more definitive assignment.

present when N_2 is used as the precursor instead of NO. Very strong ion signals corresponding to each of the isotopes of Kr are observed in the TOF spectrum every time we tune to this wavelength. This is the wavelength for the Kr one photon resonance line corresponding to the $4s^24p^5(^2P^o_{3/2})8d\ ^2[1/2]^o_1 \leftarrow {}^1S_0$ transition. When CO is used instead of NO in the beam an enhancement of the C^+, O^+, and CO^+ signals in the TOF flight spectrum is also observed at this wavelength. These observations suggest that some of the Kr gas from the four-wave mixing chamber leaks into the PD/PI region and that this gas should be responsible for the enhanced ionization that is observed in all of these gases at this wavelength. It could be due to the enhanced Kr radiation in the PD/PI region because of radiation diffusion,[54] it could also be due to collisions of atoms and molecules in the PD/PI region with either Kr^+ ions or excited Kr Rydberg atoms. At the present time we cannot eliminate any of these possible scenarios. The other peaks at 110 287 cm^{-1}, 110 296 cm^{-1}, and 110 305 cm^{-1} come from the autoionization of $N(^2D^o)$ produced in the photolysis of NO at these three wavelengths. The peak positions, effective quantum numbers and possible assignments have been listed in Table II.

Images were taken at the three autoionization lines of the $N(^2D^o)$ atom formed by the VUV photodissociation of NO. In order to do this, the VUV laser is scanned over the Doppler profile of the line while accumulating the image. The time-slice velocity-map images and their corresponding total kinetic energy release (TKER) spectra are showed Figs. 4(a)–4(f). In each of the images, three rings are observed that correspond to three peaks in each of the TKER spectra at 4.86 eV, 2.89 eV and 0.70 eV, respectively. The bond dissociation energy of NO has been reported to be 6.497 eV.[55] The three peaks in the TKER spectra can be assigned to the dissociation channels that produce $O(^3P^o)$, $O(^1D_2{}^o)$, and $O(^1S^o)$ together with $N(^2D^o)$ following the absorption of a single sum-frequency VUV photon. Besides the three main peaks, there are extra peaks at 3.62 eV, 0.16 eV, and 0.06 eV, which become more obvious in the image obtained at 110 286.7 cm^{-1} (13.6738 eV). Again, we cannot unambiguously identify these extra peaks but they could be due to the dissociation of the NO dimer to produce $NO_2 + N(^2D^o)$ as discussed earlier. These peaks are much weaker than the low energy peaks that are observed when we were detecting the $O(^1D_2{}^o)$ or $O(^3P^o)$. This is in accord with our TOF spectra which showed that the $NO_2{}^+$ peak is about a factor of 7 less than that of the N_2O^+signal.

The anisotropy parameters for the three dissociation channels at the three VUV photon energies were measured and listed in Table III. Each of the recoil anisotropy parameters represents averages of four independent measurements. The dissociation channel corresponding to $O(^3P^o)$ has a negative recoil anisotropy parameter that increases to a peak at 110 296.5 cm^{-1} and decreases after that. The $O(^1D_2{}^o)$ channel is almost isotropic at 110 286.7 cm^{-1} and becomes almost completely anisotropic with a recoil anisotropy parameter very close to −1 at 110 305 cm^{-1}. Finally, the highest energy channel, the $O(^1S^o)$ channel, is almost completely isotropic at all wavelengths. The fact that most of the β parameters are negative indicates that it is a perpendicular transition involved in the dissociation. The dissociation is also relatively fast for the $O(^3P^o)$ and $O(^1D_2{}^o)$ channels. The fact that the dissociation channel producing $O(^1S^o)$ has the β parameter very close to zero indicates that the predissociation process is slower for the $O(^1S^o)$ channel than it is for the $O(^3P^o)$ and $O(^1D_2{}^o)$ channels. Figures 4(a)–4(e) suggest that the branching ratio into each of the dissociation channels depends on the VUV photon energy. The ratio between channels $O(^1D_2{}^o)$ and $O(^3P^o)$ is about half in Fig. 4(a), but goes to nearly unity in Fig. 4(c). These changes in the dynamics are even more remarkable considering that they are occurring over a total energy span of only 18 cm^{-1}. Since we currently have only one unfocused tunable VUV beam, this does not provide enough flexibility to systematically determine the dependence of the branching ratios on the VUV photon energy. Nevertheless, we have determined the branching ratios for the three different energies and they are reported in Table III.

C. Detection of the $O(^3P_2)$ and $O(^3P_1)$ fragments

The energy of the sum-frequency VUV is below the ionization threshold of $O(^3P^o)$ atoms. To probe the $O(^3P^o)$ atoms

TABLE III. Recoil anisotropy parameters and branching ratios for the dissociation channels by probing $N(^2D^o)$.

	$N(^2D^o) + O(^3P^o)$		$N(^2D^o) + O(^1D^o)$		$N(^2D^o) + O(^1S^o)$	
VUV (cm^{-1})	β parameter[a]	Percentage (%)	β parameter	Percentage (%)	β parameter	Percentage (%)
110286.7	-0.46 ± 0.08[b]	43.1 ± 2.7	-0.17 ± 0.08	22.6 ± 1.2	0.03 ± 0.05	34.3 ± 3.8
110296.5	-0.69 ± 0.03	51.7 ± 1.3	-0.78 ± 0.01	45.3 ± 0.8	0.01 ± 0.03	3.0 ± 1.2
110305.0	-0.58 ± 0.04	70.1 ± 0.8	-0.87 ± 0.03	27.7 ± 0.7	0.15 ± 0.11	1.2 ± 0.5

[a]The equation $I(\theta) = (\sigma/4\pi)[1 + \beta P_2(\cos\theta)]$ was used to fit the experimental data to get β values.
[b]The standard deviations were generated from four independent measurements.

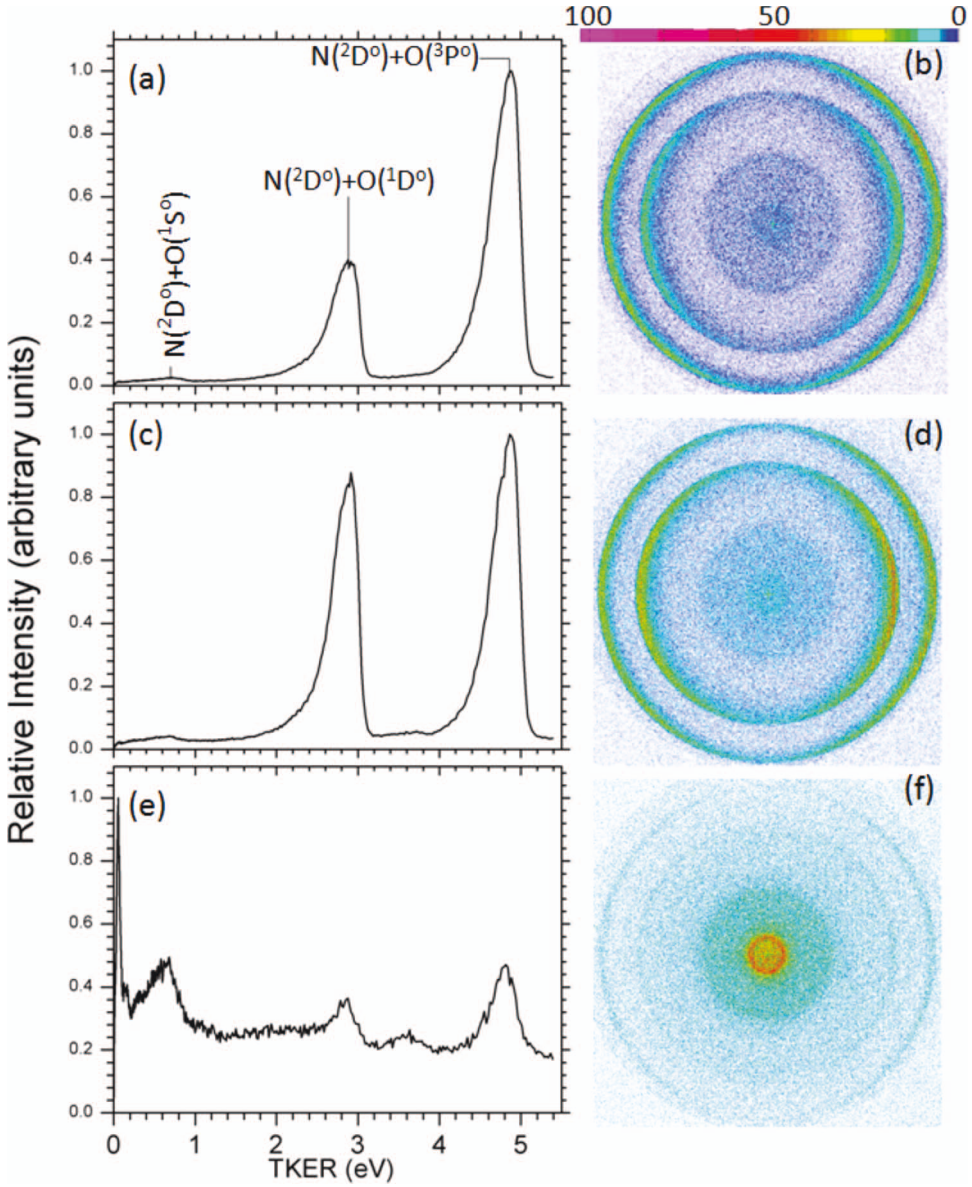

FIG. 4. Time-slice velocity-map ion images of NO by probing $N(^2D^o)$ and their corresponding total kinetic energy release (TKER) spectra. (a) and (b) 110 305.0 cm^{-1} (13.6761 eV); (c) and (d) 110 296.5 cm^{-1} (13.6751 eV); (e) and (f) 110 286.7 cm^{-1} (13.6738 eV). The VUV was scanned to cover the whole Doppler profile.

produced in the dissociation of NO, the energy of the sum-frequency VUV is tuned to one of the single photon resonance lines of $O(^3P^o)$. Subsequent absorption of a visible or UV photon will ionize the excited oxygen atom. This $1 + 1'$ ionization scheme to probe $O(^3P^o)$ can be accomplished even with unfocused lasers and it can be attributed to the large excitation cross section for the first step. With this scheme we were able to collect velocity-map ion images of $O(^3P^o)$ produced from the photodissociation of NO at the wavelengths of the $O(^3P^o)$ resonance lines. The single photon transitions at 106 766.0 cm^{-1} (13.2373 eV) ($2s^22p^3(^4S^\circ)6d\ ^3D^\circ \leftarrow {}^3P_2$) and at 107 583.9 cm^{-1} (13.3387 eV) ($2s^22p^3(^4S^\circ)7d^3D^\circ \leftarrow {}^3P_2$) of $O(^3P^o)$ were used for this purpose. Examples of the total kinetic energy release spectra are showed in Fig. 5. The solid line and solid dots spectra were collected by tuning the sum-frequency VUV to cover the Doppler profiles of the single photon transition to the oxygen state $2s^22p^3(^4S^\circ)7d^3D^\circ$ from the $O(^3P_2)$ and $O(^3P_1)$ states at VUV photon energies of 107 583.9 cm^{-1} (13.3387 eV) and 107 425.0 cm^{-1} (13.3190 eV), respectively. The transition from $O(^3P_0)$ at VUV photon energy of 107 355.6 cm^{-1} (13.3104 eV) was also seen, but it is too weak to obtain a good ion image. The open circles spectrum was collected at the VUV photon energy of 106 766.0 cm^{-1} (13.2373 eV), which is due to the transition of $2s^22p^3(^4S^\circ)6d\ ^3D^\circ \leftarrow {}^3P_2$. The transitions from $^3P_1$ and $^3P_0$ can also be seen in our oxygen ion yield spectrum (not showed here) at VUV photon energies of 106 607.9 cm^{-1} (13.2177 eV) and 106 539.4 cm^{-1} (13.2092 eV) respectively, but their intensities are not high enough to collect good ion images.

From the spectra at VUV photon energies of 107 583.9 cm^{-1} (13.3387 eV) and 107 425.0 cm^{-1} (13.3190 eV), two peaks with kinetic energies of 4.50 eV and 3.30 eV can be assigned as the dissociation channels

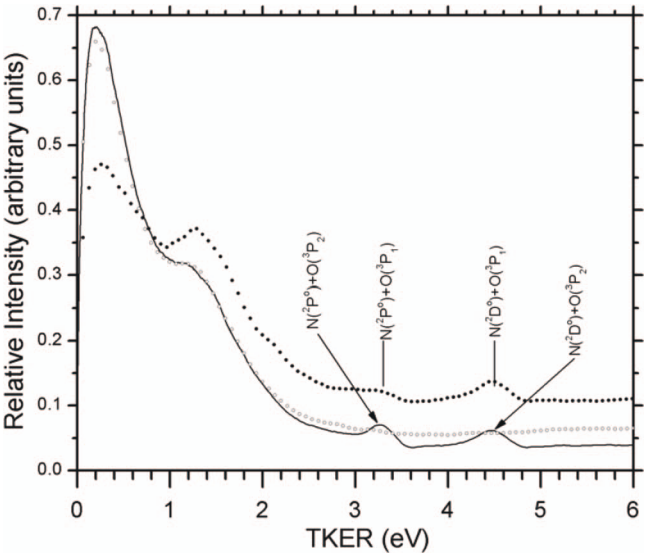

FIG. 5. Total kinetic energy release, TKER, spectra are measured by probing $O(^3P^o)$ using a $1+1'$ ionization scheme. Solid line: $2s^2 2p^3(^4S^\circ)7d^3D^\circ \leftarrow {}^3P_2$ at 107 583.9 cm^{-1} (13.3387 eV); solid dots: $2s^2 2p^3(^4S^\circ)7d^3D^\circ \leftarrow {}^3P_1$ at 107 425.0 cm^{-1} (13.3190 eV); and open circles: $2s^2 2p^3(^4S^\circ)6d^3D^\circ \leftarrow {}^3P_2$ at 106 766.0 cm^{-1} (13.2373 eV). The two dissociation channels $N(^2D^o)+O(^3P^o)$ and $N(^2P^o)+O(^3P^o)$ at total kinetic energy release of 4.50 eV and 3.30 eV, respectively, are showed in the figure.

producing $N(^2D^o) + O(^3P^o)$ and $N(^2P^o) + O(^3P^o)$, respectively, following the absorption of a single sum-frequency VUV photon by NO. These two dissociation channels cannot be seen in the spectrum obtained at the VUV photon energy of 106 766.0 cm^{-1} (13.2373 eV) (open circle spectrum in Fig. 5). Watanabe's measurements[15] of the absorption cross sections showed that it dropped by a factor of two at the longer wavelength and the percentage of dissociation is also slightly smaller. This is consistent with Metzger's measurement[14] where the photodissociation cross section decreases with decreasing photon energy. Both of these two dissociation channels again show very strong perpendicular distributions, which imply a fast dissociation process following a perpendicular transition. The strong and broad structure with relatively low kinetic energy release does not depend on the VUV photon energy, as confirmed by the fact that the solid line and open circles spectra overlap with each other in the low energy region. The spacing between the low energy peaks is about 1.0 eV, which is very close to the spacing between $N(^2P^o)$ and $N(^2D^o)$. This is likely due to the photodissociation of the NO dimer into these two channels with a small amount of energy transferred to the residual NO fragment.

IV. DISCUSSION AND CONCLUSIONS

As discussed in the introduction section, there have been many experimental studies focusing on the neutral superexcited states of NO, but the detailed energy level structures and their assignments in the energy region around 13.5 eV above the ground state are still unknown because of the lack of theoretical calculations. In 1966, Metzger *et al.*[14] reported a broad dissociative band that peaks at 91 nm. The branching ratio in this energy region between photoionization and photodissociation was determined by both Metzger *et al.*[14] and Watanabe *et al.*[15] High resolution measurements of the absolute optical oscillator strengths for photoabsorption of NO from 5 eV to 30 eV were reported by Chan *et al.*[18] in 1993. Li and co-workers repeated the absolute optical oscillator strengths measurement in the region from 5.0 to 22.0 eV by using a high-resolution fast-electron energy loss spectrometer in 2002.[21] These two measurements agree with each other and both showed a broadened continuum underneath complicated sharp resonant peak structures around 13.5 eV. Zhong *et al.* have used their high resolution energy loss spectrum and quantum defect theory to assign the electronic states responsible for the spectrum in the region that we are studying.[20] Their assignments suggest that the absorption in this region is due to an excitation of an electron from 1π to 2π orbital resulting in a Π-Π transition. The transition is from the ground vibronic state of NO $X^2\Pi$ ($\pi^4\pi^{*1}$) to the highly excited vibrational levels of the $L^2\Pi$ ($\pi^3\pi^{*2}$) state and it can be written as $L^2\Pi$-$X^2\Pi$ ($v' > 11$, $v = 0$). In fact, according to Fig. 1 in Zhong's paper, both of the $B^2\Pi$ and $L^2\Pi$ states contribute to the absorption in this energy region. They calculated the absolute optical oscillator strengths to insure that theoretical transition probabilities agree with the experimental measurements. They also assigned each of the sharp resonant peaks in this region to Rydberg states converging to the excited NO ionic states. The experimental recoil anisotropy parameters are strongly dependent on the symmetry of the excited state. Recoil anisotropy parameters of -1 and 2 correspond to pure perpendicular and parallel transitions, respectively following a fast dissociation process. All values between -1 and 2 indicate a deviation from the two extreme cases, either the transition is a mixture of both perpendicular and parallel transitions or the dissociation is not fast compared with the rotation of the molecule.[56] Tables I and III show that, except for the $N(^2D^o) + O(^1S^o)$ channel, all of the recoil anisotropy parameters are negative and that most of them are very close to -1. This indicates that the transition is largely perpendicular with an upper state of either Σ or Δ symmetry.[57] It should go toward zero if the dissociation is slower or if a state with Π symmetry is involved in the dissociation. This is contrary to the previous assignments reported by Zhong *et al.*[20] in this region. Without quantitative theoretical calculations, we cannot unambiguously identify the specific states involved in the dissociation in this region, but the valence states $I\,{}^2\Sigma^+$ and $B'\,{}^2\Delta$ are among the best possible candidates in this energy region according to the theoretical calculations of Vivie and Peyerimhoff.[10] Both of these two valence states converge to the $N(^2D^o) + O(^3P^o)$ limit, the equilibrium positions of their potential curves are larger than that of the ground state and a little smaller than that of $B^2\Pi$ and $L^2\Pi$ states. The Frank-Condon factors in this region should be largely based on Zhong's calculation about the $B^2\Pi$ and $L^2\Pi$ states. In fact our conclusion about the symmetries of the electronic states in this region supports the results of the experimental and theoretical studies of Erman *et al.*[58] According to their theoretical calculations using the many-body theory, the electronic states with Σ and Δ symmetries dominate the electric dipole transition probabilities for NO in the energy region of the present study. The transition

probabilities to electronic states with Π symmetry are all very small in this region.

Other possible candidates that could be responsible for our results are Rydberg states with Σ or Δ symmetry in this region. The Rydberg states can couple to the valence states, which then leads to predissociation to the observed products. Theoretical calculations by Sun *et al.*[59] and Schneider *et al.*[60] on the dissociative recombination cross section of NO^+ showed that such an interaction is important. The Rydberg-valence interactions in this region have also been reported by Sobolewski[61] and Erman *et al.*[58] Another less likely reason why we observed minus recoil anisotropy parameters is due to a complicated predissociation mechanism following a Π-Π transition. Buijsse and co-workers observed a recoil anisotropy parameter of about 1.2 for the dissociation channel $N(^4S) + N(^2P)$ of N_2 following the transition of $N_2(e^1\Pi_u, v' = 0, J' = 2) \leftarrow N_2(a''^1\Sigma_g^+, v'' = 0, J'' = 1)$ which should be a pure perpendicular transition.[62] This observation shows that the predissociation mechanism can alter the originally alignment of the molecules by a linearly polarized laser. The measured recoil anisotropy parameters deviated from the extreme value of minus one, which implies that this region also has partially Π character.

If the excitation of NO in this energy region is due to the $X\ ^2\Pi \rightarrow B^2\Pi$ and/or $L^2\Pi$ transition then mixing with a Σ or Δ state must be occurring in order to explain the present results. The fact that no rotational structure has been resolved in the observed spectra of NO in this region indicates that dissociation lifetimes here are considerably shorter than the rotational period, in fact lifetimes of the order of femtoseconds have been obtained by Erman *et al.*[58] A lifetime this short means that the rotation of the molecules cannot dramatically affect the angular distribution of the nascent products.

All the energetically available photodissociation channels of NO below 15 eV have been listed in Fig. 6. Previous multi-photon excitation studies of NO in the vicinity of its first ionization threshold have identified the photodissociation channels producing $O(^3P) + N(^4S)$, $O(^3P) + N(^2D)$, and $O(^1D_2) + N(^4S)$. To the best of our knowledge, the channels with slightly higher dissociation energies like $N(^2D^o) + O(^1D_2)$, $N(^2D^o) + O(^1S_0)$, and $N(^2P^o) + O(^3P)$ have never been reported before because there was not enough photon energy to produce them. Here with the single VUV photon excitation method, we have enough energy to see all these dissociation channels. Some of the energetic available channels like $N(^2P^o) + O(^1D_2{}^o)$ and $N(^4S^o) + O(^1D_2{}^o)$ are not seen here. The latter channel is spin forbidden but we have observed spin forbidden channels in both N_2 (Ref. 40) and CO (Ref. 63) indicating that the spin selection rule is not as important in this high energy region. More experimental and theoretical work is needed to understand why these channels have not been observed in NO.

Our experimental results have also been used to observe and assign autoionization lines for the $O(^1D_2{}^o)$ and $N(^2D^o)$ atoms. These are useful for specifically monitoring a particular state of the oxygen or nitrogen atom as the wavelength of the dissociation laser is changed. The present results show that the images can be used to study the dynamics of photodissociation of dimers and clusters but systematic studies of this and the monomer will require an apparatus that has the flexibility to independently vary the photolysis wavelength and simultaneously detect a particular atomic fragment.

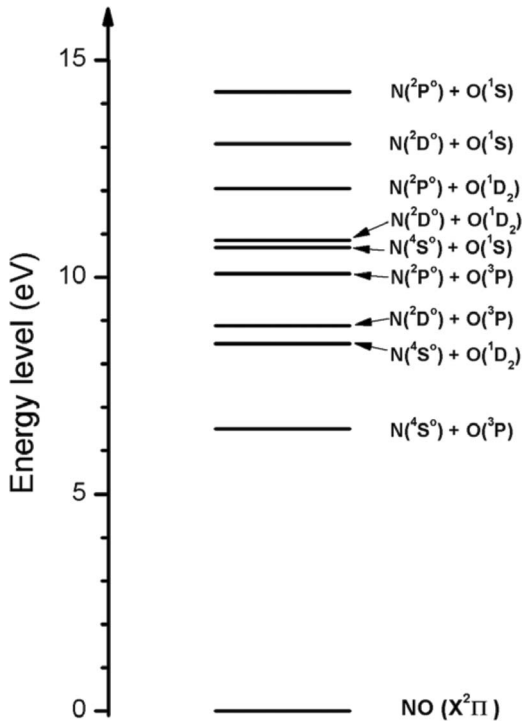

FIG. 6. Energy diagram for all the dissociation channels of NO below 15 eV.

In summary, a direct single VUV photon photodissociation study of NO in the energy region around 13.5 eV has been done using time-slice velocity-map ion imaging technique. This is the first time that a direct photodissociation study has been done for NO in this energy region. Probing the $N(^2D^o)$, $O(^3P)$, and $O(^1D_2)$ photofragments at several different VUV photon energies has allowed us to identify new photodissociation channels that produce $N(^2D^o) + O(^1D_2)$, $N(^2D^o) + O(^1S_0)$, and $N(^2P^o) + O(^3P)$. We have been able to determine the total kinetic energy release and the corresponding angular distributions of these photodissociation channels. Most of the dissociation channels show strong anisotropic perpendicular angular distribution with negative recoil anisotropy parameters. This implies that the excited states leading to the photodissociation have Σ or Δ symmetry. While this is contrary to the previous assignments of Π symmetry made by Zhong *et al.*[20] it agrees with the conclusion of Erman *et al.*[58]

ACKNOWLEDGMENTS

H. Gao, Y. Pan, and W. M. Jackson were supported by NSF under Grant No. CHE-0957872. H. Gao, L. Yang, Jingang Zhou, and C. Y. Ng were supported by AFOSR under Grant No. FA9550-06-1-0073, NASA under Grant No. 07-PATM07-0012, DOE on Contract No. DEFG02-02ER15306, and NSF on Grant No. CHE 0910488.

[1]D. R. Bates and M. J. Seaton, Proc. Phys. Soc. London **B63**, 129 (1950).
[2]P. G. Richards, D. G. Torr, and M. R. Torr, J. Geophys. Res. **86**, 1495, doi:10.1029/JA086iA03p01495 (1981); S. Solomon, Planet. Space Sci. **31**, 135 (1983).
[3]D. G. Steyn, J. W. Bottenheim, and R. B. Thomson, Atmos. Environ. **31**(14), 2025 (1997).
[4]H. S. Liszt and B. E. Turner, Astrophys. J. **224**, L73 (1978).
[5]J. Daranlot, M. Jorfi, C. Xie, A. Bergeat, M. Costes, P. Caubet, D. Xie, H. Guo, P. Honvault, and K. M. Hickson, Science **334**(6062), 1538 (2011).
[6]K. Dressler and E. Miescher, Astrophys. J. **141**, 1266 (1965).
[7]E. Miescher, J. Mol. Spectrosc. **20**, 130 (1966).
[8]E. Miescher, Can. J. Phys. **54**, 2074 (1976); E. Miescher and F. Alberti, J. Phys. Chem. Ref. Data **5**(2), 309 (1976).
[9]R. Gallusser and K. Dressler, J. Chem. Phys. **76**, 4311 (1982).
[10]R. de Vivie and S. D. Peyerimhoff, J. Chem. Phys. **89**, 3028 (1988).
[11]R. Polak and J. Fiser, Chem. Phys. Lett. **377**, 564 (2003).
[12]H. C. Shi and A. L. L. East, J. Chem. Phys. **125**, 104311 (2006).
[13]H. Sun and G. L. Weissler, J. Chem. Phys. **23**, 1372 (1955).
[14]P. H. Metzger, G. R. Cook, and M. Ogawa, Can. J. Phys. **45**, 203 (1967).
[15]K. Watanabe, F. M. Matsumaga, and M. Sakai, Appl. Opt. **6**, 391 (1967).
[16]D. L. Albritton, A. L. Schmeltekopf, and R. N. Zare, J. Chem. Phys. **71**(8), 3271 (1979).
[17]R. J. Stubbs, T. A. York, and J. Comer, Chem. Phys. **106**, 161 (1986).
[18]W. F. Chan, G. Cooper, and C. E. Brion, Chem. Phys. **170**, 111 (1993).
[19]P. Erman, A. Karawajczyk, E. Rachlew-Kallne, and C. Stromholm, J. Chem. Phys. **102**, 3064 (1994).
[20]Z. P. Zhong, W. H. Zhang, and J. M. Li, J. Chem. Phys. **113**, 136 (2000).
[21]L. F. Zhu, Z. P. Zhong, Z. S. Yuan, W. H. Zhang, X. J. Liu, X. M. Jiang, K. Z. Xu, and J. M. Li, Chin. Phys. **11**, 1149 (2002).
[22]G. K. Jarvis, Y. Song, and C. Y. Ng, J. Chem. Phys. **111**, 1937 (1999).
[23]G. K. Jarvis, M. Evans, C. Y. Ng, and K. Mitsuke, J. Chem. Phys. **111**, 3058 (1999).
[24]J. Berkowitz, *Atomic and Molecular Photoabsorption: Absolute Total Cross Sections*, 1st ed. (Academic, San Diego, 2001).
[25]L. E. Jusinski, G. E. Gadd, G. Black, and T. G. Slanger, J. Chem. Phys. **90**, 4282 (1989).
[26]G. E. Gadd, L. E. Jusinski, and T. G. Slanger, J. Chem. Phys. **91**, 3378 (1989).
[27]A. Fujii and N. Morita, Chem. Phys. Lett. **182**, 304 (1991).
[28]A. Fujii and N. Morita, J. Chem. Phys. **97**, 327 (1992).
[29]A. Fujii and N. Morita, J. Chem. Phys. **98**, 4581 (1993).
[30]B. L. G. Bakker, A. T. J. B. Eppink, D. H. Parker, M. L. Costen, G. Hancock, and G. A. D. Ritchie, Chem. Phys. Lett. **283**, 319 (1998).
[31]B. L. G. Bakker, D. H. Parker, G. Hancock, and G. A. D. Ritchie, Chem. Phys. Lett. **294**, 565 (1998).
[32]B. R. Cosofret, H. M. Lambert, and P. L. Houston, J. Chem. Phys. **117**, 8787 (2002).
[33]A. Ehresmann, H. Liebel, M. von Kroger, and H. Schmoranzer, J. Phys. B **34**, 2893 (2001).
[34]A. Ehresmann, H. Liebel, M. von Kroger, and H. Schmoranzer, J. Phys. B **34**, 3119 (2001).
[35]E. M. Carcia, J. A. Ruiz, P. Erman, A. Kivimaki, E. R. Kallne, J. R. Riu, M. Stankiewicz, and L. Veseth, Chem. Phys. **293**, 65 (2003).
[36]Y. Hikosaka, T. Aoto, K. Ito, Y. Terasaka, R. Hirayama, and E. Miyoshi, J. Chem. Phys. **128**, 044320 (2008).
[37]H. Oertel, H. Schenk, and H. Baumgartel, Chem. Phys. **46**, 251 (1979).
[38]J. H. D. Eland and E. J. Duerr, Chem. Phys. **229**, 1 (1998).
[39]Y. Pan, H. Gao, L. Yang, J. Zhou, C. Y. Ng, and W. M. Jackson, J. Chem. Phys. Commun. **135**, 071101 (2011).
[40]H. Gao, L. Yang, Y. Pan, J. Zhou, C. Y. Ng, and W. M. Jackson, J. Chem. Phys. **135**, 134319 (2011).
[41]E. Wigner and E. E. Witmer, Z. Phys. A: Hadrons Nucl. **51**(11), 859 (1928).
[42]J. G. Zhou, K. C. Lau, E. Hassanein, H. F. Xu, S. X. Tian, B. Jones, and C. Y. Ng, J. Chem. Phys. **124**, 034309 (2006).
[43]J. G. Zhou, B. Jones, X. L. Yang, W. M. Jackson, and C. Y. Ng, J. Chem. Phys. **128**, 014305 (2008).
[44]B. Jones, J. G. Zhou, L. Yang, and C. Y. Ng, Rev. Sci. Instrum. **79**, 123106 (2008).
[45]R. Flesch, M. C. Schurmann, J. Plenge, H. Meiss, M. Hunnekuhl, and E. Ruhl, Phys. Rev. A **62**, 052723 (2000).
[46]R. N. Clayton, Nature (London) **415**(6874), 860 (2002).
[47]H. Reisler, Annu. Rev. Phys. Chem. **60**, 39 (2009).
[48]O. Geßner, A. M. D. Lee, J. P. Shaffer, H. Reisler, S. V. Levchenko, A. I. Krylov, J. G. Underwood, H. Shi, A. L. L. East, D. M. Wardlaw, E. t.H. Chrysostom, C. C. Hayden, and A. Stolow, Science **311**(5758), 219 (2006).
[49]C. J. Zeippen, M. L. Dourneuf, and V. K. Lan, J. Phys. B **13**, 3763 (1980).
[50]K. L. Bell, K. A. Berrington, and C. A. Ramsbottom, J. Phys. B **25**, 1209 (1992).
[51]V. Cermak, J. Electron Spectrosc. Relat. Phenom. **3**, 329 (1974).
[52]S. Boumsellek and V. A. Esaulov, J. Phys. B **23**, L605 (1990).
[53]Y. Hikosaka, H. Hattori, T. Hikida, and K. Mitsuke, J. Chem. Phys. **105**, 6367 (1996).
[54]A. C. G. MITCHELL and M. W. ZEMANSKY, *Resonance Radiation and Excited Atoms*, 1st ed. (Cambridge University Press, 1971).
[55]P. Huber and G. Herzberg, *Molecular Spectra and Molecular Structure* (Van Nostrand, Princeton, 1979).
[56]B. J. Whitaker, *Imaging in Molecular Dynamics: Technology and Application*. (Cambridge University Press, 2003).
[57]R. N. Zare and D. R. Herschbach, Proc. IEEE **51**, 173 (1963).
[58]P. Erman, A. Karawajczyk, E. Rachlew-Källne, M. Stankiewicz, K. Yoshiki Franzén, P. Sannes, and L. Veseth, Chem. Phys. Lett. **273**(3–4), 239 (1997).
[59]H. Sun and H. Nakamura, J. Chem. Phys. **93**, 6491 (1990).
[60]I. F. Schneider, I. Rabadan, L. Carata, L. H. Andersen, A. S. Weiner, and J. Tennyson, J. Phys. B **33**, 4849 (2000).
[61]A. L. Sobolewski, J. Chem. Phys. **87** (1), 331 (1987).
[62]B. Buijsse and W. J. v. d. Zande, J. Chem. Phys. **107**, 9447 (1997).
[63]H. Gao, Y. Song, L. Yang, X. Shi, Q. Yin, C. Y. Ng, and W. M. Jackson, J. Chem. Phys. **135**(22), 221101 (2011).